Journal of Magnetic Resonance 203 (2010) 311–315

Contents lists available at ScienceDirect

Journal of Magnetic Resonance

journal homepage: www.elsevier.com/locate/jmr

Communication

Single-scan 2D NMR correlations by multiple coherence transfers

Maayan Gal [1], Lucio Frydman *

Department of Chemical Physics, Weizmann Institute of Science, Rehovot 76100, Israel

ARTICLE INFO

Article history:
Received 27 October 2009
Available online 3 November 2009

Keywords:
Multidimensional spectroscopy
Ultrafast 2D NMR
HSQC
Coherence transfer processes

ABSTRACT

A new scheme for the acquisition of heteronuclear 2D correlations in NMR spectroscopy within a single scan, is proposed and demonstrated. The principles of this new scheme resemble those of Mansfield's "*k*-space walk" proposal, in the sense that they rely on repetitively transferring spin coherences back-and-forth between the two spin systems to be correlated. It is shown that if properly executed, these transfers enable the equivalent of a continuous sampling of the time-domain space supporting a 2D heteronuclear single-quantum correlation NMR spectrum. Details on how to execute the resulting "time-domain walk" experiments are given, and examples comparing it against conventional and other single-scan 2D acquisition alternatives are shown. Advantages, opportunities, and main drawbacks of this new ultrafast approach to 2D NMR, are briefly discussed.

© 2009 Elsevier Inc. All rights reserved.

Nuclear Magnetic Resonance (NMR) provides one of the most versatile tools available for analyzing structure, function and dynamics at a molecular level [1]. Benefiting from this information requires resolving and assigning each spectral peak to its corresponding atomic site; tasks in which two-dimensional (2D) NMR plays an important role [2,3]. 2D NMR typically relies on mapping two frequencies, arising for instance from a $^{13}C/^{15}N$ and from a J-coupled ^{1}H, by encoding them along two different time domains [4,5]. One of these domains, t_2, involves a physical acquisition and can be probed within a sub-second timescale. By contrast the other time-domain, t_1, is usually monitored by incrementing an evolution delay within a pulse sequence on a scan-by-scan basis. This implies that, regardless of sensitivity considerations, 2D NMR acquisitions may demand the collection of several scans just for satisfying Nyquist-related criteria; in certain sampling-limited cases, this may lead to much longer acquisition times than for their 1D counterparts. Recent years have witnessed extensive efforts geared at bypassing this built-in, multi-scan feature of 2D NMR acquisitions [6–9]. The resulting methods are playing increasingly important roles, particularly in challenging biostructural settings [10–12]. These schemes can be divided into approaches which reduce the number of needed scans by virtue of a non-Fourier processing of conventionally-collected data [6,7], and those which depart from classical schemes to do the 2D NMR acquisition [8,9]. Counted among the latter are so-called spatially-encoded experiments, capable of compressing arbitrary 2D NMR acquisitions into a single scan [13–15]. Although inspired by Mansfield's proposition for the echo-planar acquisition of 2D NMR images [16,17], the physical principles underlying these "ultrafast" spectroscopic schemes are different. Ultrafast 2D NMR relies on encoding the indirect-domain evolution frequencies along spatial rather than temporal domains; echo-planar-imaging by contrast, involves oscillating the gradients used to encode the spins' positions back-and-forth, so as to transverse a full 2D plane of the Fourier-conjugate imaging *k*-space within a single scan. Such "walk" through *k*-space [18] requires a flexibility that, in general, is rarely available in spectroscopy-oriented NMR experiments [19–22]. Still, this work introduces the equivalent of a "time-domain walk" approach capable of yielding, in a single scan, all the information needed to establish 2D correlations within coupled heteronuclear spin systems.

For concreteness we consider a heteronuclear single-quantum correlation (HSQC) experiment, aimed at jointly measuring the frequencies characterizing a X–^{1}H spin-pair based on J-mediated coherence transfer processes [1–3,23]. The typical HSQC would achieve this by using an INEPT-type block [24] to relay the X evolution encoded over a time t_1 onto a neighboring ^{1}H, whose signal would then be detected as a function of a time t_2. Further refinements like preceding the overall experiment with a pre-polarizing transfer from the more highly aligned ^{1}Hs to the X spins, or transferring both quadrature components of the X spin evolution back to the ^{1}Hs for an enhanced sensitivity [25], could also be included. The main principle of the method hereby discussed rests on iterating on these two latter approaches; i.e., in periodically transferring both components making up single-quantum coherences in such systems from the ^{1}Hs to the coupled X spins, back-and-forth multiple times, following a single excitation of the spin ensemble. If properly executed, the evolution of ^{1}H–X spin pairs acted upon

* Corresponding author. Fax: +972 8 9344123.
E-mail address: lucio.frydman@weizmann.ac.il (L. Frydman).
[1] Present address: Department of Biological Chemistry and Molecular Pharmacology, Harvard Medical School, Boston, MA 02115, USA.

1090-7807/$ - see front matter © 2009 Elsevier Inc. All rights reserved.
doi:10.1016/j.jmr.2009.10.013

by such sequence can then be described by a trajectory in a joint 2D (t_X,t_H)-space, where t_X describes the chemical shift evolution imparted on the common spin coherences by the X spin, whereas t_H does the same for its coupled proton. Suitable sampling of the spins' response while undergoing such "time-walk", followed by appropriate rearrangement of the digitized data and conventional 2D Fourier processing, can then lead to heteronuclear 2D NMR correlation spectra comparable to those arising from conventional acquisitions – but without the need to increment a t_1 parameter throughout multiple scans. Fig. 1 illustrates this capability for the case of ^{1}H–^{13}C 2D correlations on a natural abundance, concentrated (≈50% w/w) sample. Fig. 2 presents a similar illustration, but for the case of a 2D ^{1}H–^{15}N HSQC correlation implemented on a 2 mM tripeptide. In both instances, representative cross-sections illustrating the relative sensitivity and resolution of the methodology, are shown.

Fig. 3 shows a hierarchical description of the principles leading to this new kind of data acquisition, at different levels of detail. Panels 3A and B indicate the trajectory imposed by the sequence on the spins as viewed in the (t_X,t_H)-space: according to this convention a horizontal displacement will occur whenever coherences evolve under the effects of the ^{1}H's shift, an X-shift evolution will impose a vertical displacement, and a spin echo (i.e., reversing one of the spin-coherence quadrature components while leaving the second unaffected) corresponds to reflecting the instantaneous (t_X,t_H) coordinate through the origin. In order to sample this 2D space densely in a single scan, the sequence does as follows (lettering here matching with corresponding points in Fig. 3A): (a) it triggers a ^{1}H-detected evolution (for better sensitivity) lasting an interval $t_H^{max}/2$; this is in principle the only spin excitation needed to complete the full 2D acquisition. (b) It transfers the resulting state to an X single-quantum anti-phase coherence according to a $H_x \rightarrow 2H_zX_x$, $H_y \rightarrow 2H_zX_y$ sensitivity-enhanced scheme. (b → c) It allows these coherences to evolve under X's chemical shift for an interval $\Delta t_X/2$, thereby encoding X's effect and moving solely along the t_X-axis. (c → d) It transfers this X-encoded evolution back to protons according to a second $2H_zX_x \rightarrow -H_x$, $2H_zX_y \rightarrow H_y$ sensitivity-enhanced scheme acting as a sort of coherence echo. (d → e) It lets the protons evolve freely over a time t_H^{max}, while recording their signal and allowing the ensemble to evolve along the t_H-axis. (e → f) It echoes the full spin evolution by applying a ^{1}H π-pulse, which is equivalent to a reflection of the spins' evolution through the origin of the (t_H,t_X)-plane. And (g), it repeats the full (a)-(f) sequence but making now all ^{1}H and X free evolution periods t_H^{max} and Δt_X, respectively. While other alternatives can also be devised, Fig. 3B illustrates how the relevant 2D time-domain is then sampled densely with a regular array of points, arising from data being acquired whenever ^{1}H free evolution takes place: t_H thereby takes the role of the usual t_2 direct-domain, whereas Δt_X corresponds to the customary increment Δt_1. Fig. 3C and D complete this description by noting elements such as the decoupled evolution imposed along both domains, the data sampling timing, gradient-enhancement filters, and the three main heteronuclear coherence transfer blocks involved: P_1, P_2 and P_3. P_1 and P_3 are meant to execute $H_x \rightarrow 2H_zX_x$, $H_y \rightarrow 2H_zX_y$ sensitivity-enhanced-like INEPT schemes, whereas P_2 does a $2H_zX_x \rightarrow -H_x$, $2H_zX_y \rightarrow H_y$ back-transfer in combination with a coherence echo that effectively reverses the evolution in the 2D time-domain plane. Notice that both P_1 as well as the initial, shorter evolution times, play somewhat special roles owing to the initial state of the spin-pair magnetization (starting solely as H_z). While sub-optimal, neglecting these data yields a string of points that is ready to conventional FFT (e.g., red dots in Fig. 3B); phase-cycling of the pulses to suppress non-encoded ^{1}H signals is also feasible; given the quadrature, phase-sensitive transfers in-

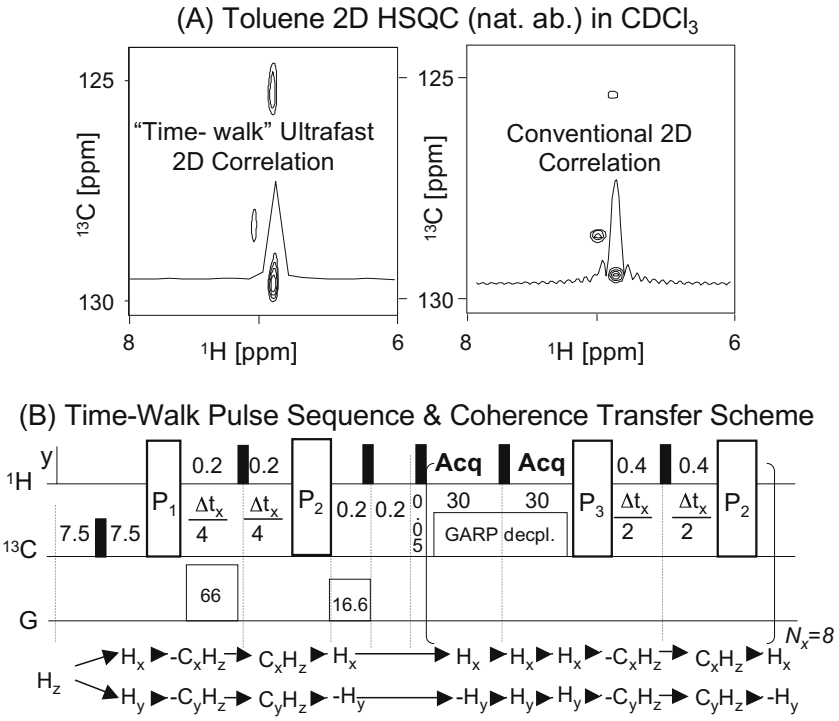

Fig. 1. (A) Comparison between the new "time-walk" heteronuclear correlation approach introduced in this work, and conventional 2D HSQC NMR results for a 50/50% Toluene/$CDCl_3$ sample. Cross-sections on one of the peaks are also shown for both 2D spectra. Data were recorded at 11.7 T using a Varian Inova® spectrometer using comparable overall evolution t_1 and acquisition t_2 times – even if the conventional 2D acquisition required 32 total scans. Linear prediction was used for all sets. (B) Sequence details for the "time-walk" experiment in part A, showing $\pi/2$ and π pulses by thin and thick lines respectively, the actual looped sampling periods denoted by ***Acq***, all delays in ms, and gradients in G/cm. The $\{P_i\}_{i=1-3}$ blocks are coherence transfer sequences, whose purposes are further explained in the text and whose precise timing (pulses, delays) is summarized in Fig. 3D. Also shown underneath the sequence are the main coherence transfer processes involved during the course of the experiment.

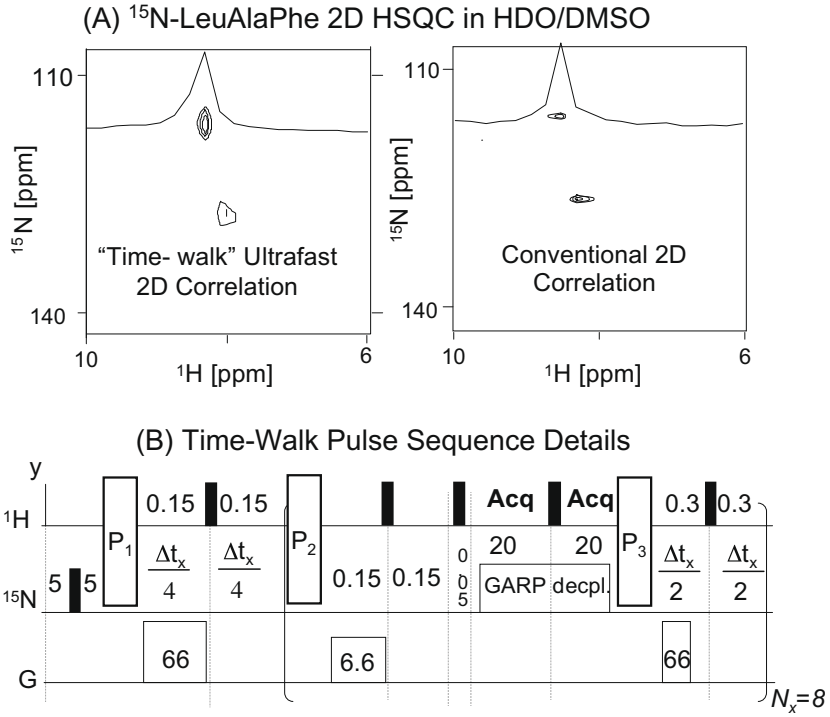

Fig. 2. (A) Idem as in Fig. 1, but for ^{1}H–^{15}N 2D heteronuclear correlation experiments recorded on a 2 mM tripeptide sample; cross-sections (magnitude) are included for comparison. (B) Summary of the new ultrafast sequence parameters employed; the conventional 2D acquisition involved 16 t_1 indirect-domain increments with a Δt_1 = 800 μs, a two-step phase cycling for each increment, a direct acquisition time of 20 ms (similar to the "time-walk" acquisitions), and coherence-selection gradients/GARP decoupling parameters with the same values/delays as in the ultrafast acquisitions.

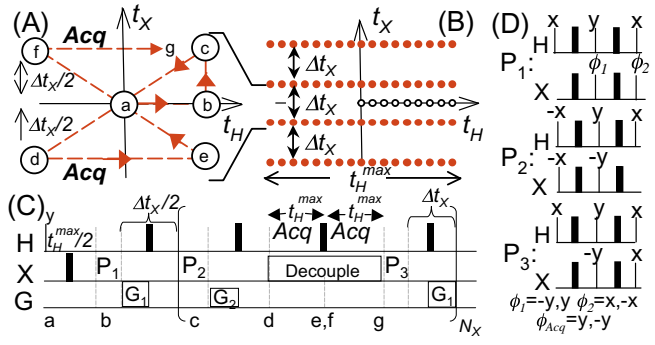

Fig. 3. Details of how the time-domain space supporting a 2D H, X heteronuclear correlation spectrum, could be scanned in a "single shot". (A) Initial zoomed-out trajectory executed by the spins in the 2D (t_X,t_H)-space that is Fourier-paired to the spectrum being sought, under the (a–g) events described in the text. (B) Sampling over the course of the experiment: except for the (hollow) data subtended between (a) and (b), all points end up distributed in a regular grid ready for fast 2D Fourier transformation. (C and D) Further details on the execution of this pulse scheme including $\pi/2$ and π (thin, thick lines) pulses, G_1, G_2 selection gradients defined by γ_X/γ_H, a minimal two-scan phase cycling, heteronuclear decoupling, and the sensitivity-enhanced coherence transfers $\{P_i\}_{i=1-3}$ specified in (D). All delays between $\pi/2$ and π pulses in these blocks are set to $0.25/J_{XH}$. (For interpretation of color mentioned in this figure, the reader is referred to the web version of this article.)

volved in the experiment this cycling is somewhat unusual, requiring simultaneous changes in two of the X-pulse $\pi/2$ transfer pulses in synchrony with a reversal of the receiver's phase, in order to implement a minimal two-scan phase alternation (Fig. 3D).

It is pertinent to highlight what we perceive are the main features associated with this new approach to single-scan 2D heteronuclear correlations. The method's main limitations probably arise from: (i) its reliance on the relatively long coherence transfer P-blocks, which will be affected by T_2-driven relaxation losses without contributing to actual observable signals; and (ii) its reliance on multiple Δt_X-increments intersparsed into the ^{1}H signal detection blocks, which will by necessity introduce compromises in the evolution times – and hence the spectral resolutions – achievable along both spectral dimensions. The first of these complications implies that the method will operate best for small molecules or for macromolecules with high internal mobility, characterized by long T_2s and large heteronuclear coupling constants. The second complication can be alleviated to an arbitrary degree at the expense of the method's single-scan character, on the basis of interleaved acquisitions – of the kind further illustrated in Fig. 4. This last Sucrose-based ^{13}C–^{1}H HSQC example also highlights what is arguably the main advantage of the new scheme over existing single-scan 2D alternatives, arising from its considerably higher sensitivity vis-à-vis spatially-encoded methods. This can be appreciated by comparing the various cross-sections illustrated in panel 4A, and can be further rationalized on the basis of the gradient-free nature of the "time-walk" acquisitions: by involving conventional dwell times and filter bandwidths these methods are thereby free, on a per scan basis, from the noise penalties associated to spatial encoding [14,15]. The absence of gradients should also be a bonus when considering experiments associated with turbulent, random-like flow; including monitoring of real-time kinetics triggered by sudden injections, or 2D NMR experiments based on *ex situ* DNP [26–28]. Another point worth mentioning, are the different behaviors that single-quantum and higher-rank spin states like those arising from H_nX systems, will exhibit when acted by these pulse schemes. Coherence transfer analyses reveal, for instance, that given the sequences implemented in Figs. 1 and 2, both amplitude-modulated and unmodulated observable terms will originate from CH_2 groups. Details on the fate of these groups are further detailed in Fig. 5. However, as can be appreciated from the insets highlighted in the Sucrose

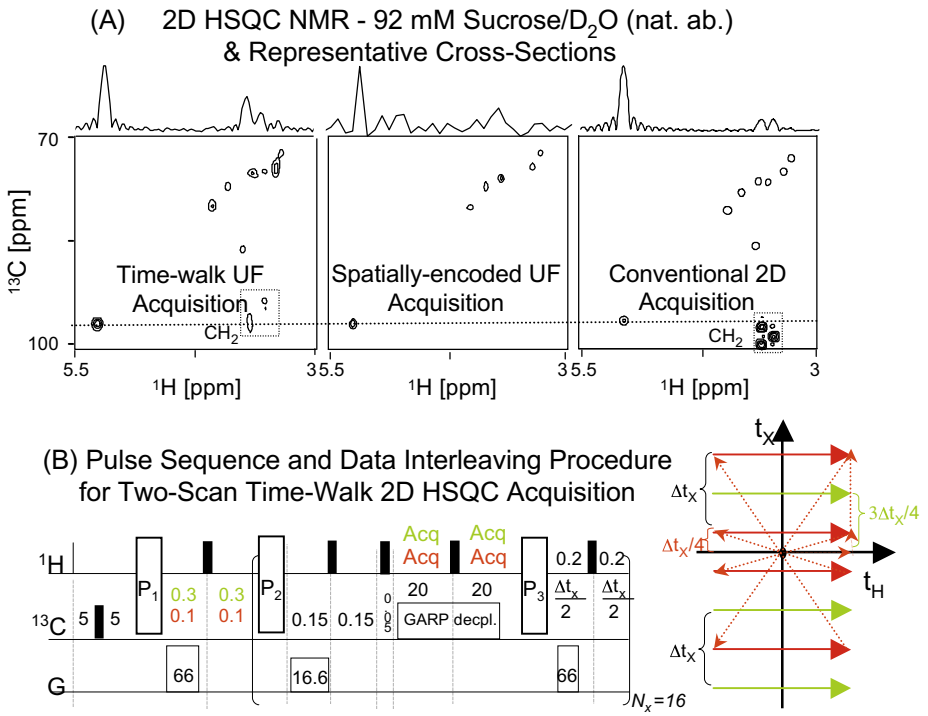

Fig. 4. (A) Comparison between ultrafast and conventional data sets collected at 14.1 T on 92 mM Sucrose/D_2O, using a Varian VNMRS® triple-resonance console. Both "ultrafast" spectra were acquired in four scans, including two interleaved sets of phase-cycled data. The conventional experiment included 2-scan phase-cycling times 32 t_1 increments; no post-processing was applied to any of the sets beyond fast Fourier transforms. As both the conventional and te "time-walk" HSQC spectra were recorded under analogous conditions (Δt_1 = 200 μs, 20 ms acquisition times, similar coherence-selection gradients and decoupling conditions, etc.), both acquisitions lead to a similar folding on the methylene cross-peaks – indicated by the dashed boxes. The spatially-encoded data set was collected using comparable spectral-width and resolution parameters along both frequency domains. Yet being based on a non-numerical Fourier transform, folding along F1 does not occur and the methylene cross-peaks are absent. Additional parameters of this experiment included a 6.4 ms long constant-time version of the 2D HSQC spatial encoding [29], 50 G/cm encoding gradients, 4 G/cm decoding (acquisition) gradients, Δt_2 = 1100 μs and the equivalent of 18 t_2 acquisition-time points. Traces on top of each spectrum correspond to 1D cross-sections extracted at the dashed-line positions, and illustrate the better sensitivity of the new ultrafast procedure vis-à-vis its spatially-encoded counterpart. (B) Sequence employed to collect the "time-walk" spectrum in panel A (delays in ms, gradients in G/cm, $\{P_i\}_{i=1-3}$ blocks as in Fig. 3D). Shown on the right is the denser coverage of the (t_X,t_H)-plane that two scans with different initial X evolution delays can provide, when suitably interleaved. In this cartoon, continuous red/green lines indicate the actual acquisition coordinates associated to the different initial red/green delays. The dotted arrows indicate the remaining "time-walk" processes associated with the red-labeled scan. Notice that upon interleaving the data sets as shown, the effective dwell along the t_X-axis ends up being halved to $\Delta t_X/2$ from its original Δt_X value. (For interpretation of color mentioned in this figure, the reader is referred to the web version of this article.)

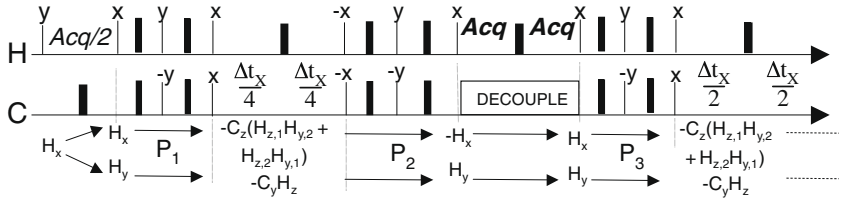

Fig. 5. Fate of CH_2 spin coherences when acted upon by the sequence introduced in Figs. 1–4 (thin and thick lines correspond to $\pi/2$ and π pulses respectively and, unless specified, interpulse delays correspond to 0.25/J). Notice that by contrast to the case of a CH spin-pair – e.g., the transfer pathways in Fig. 1 – there is a loss of quadrature evolution along t_X. Still, the sequence fully recovers the initial H_x, H_y states at the end of each cycle, and therefore no cumulative signal losses occur over the repetitive H<–>X transfer processes.

example (Fig. 4A), the resulting kind of modulations do not prevent the ultrafast collection of 2D correlations even from these higher spin systems.

In summary, we have presented a new approach for the single-scan correlation of heteronuclei. Unlike previous "ultrafast" proposals this sequence operates on the basis of "time-walk" concepts, akin to those underlying echo-planar-imaging experiments but involving solely spectroscopic evolutions. The new method requires certain compromises in terms of spectral resolution and of the relaxation times it can support; but it has the advantage of bypassing the need for encoding/decoding gradients – and their associated sensitivity penalties. From an execution and processing standpoint, the "time-walk" approach is also much more akin to conventional multi-scan 2D acquisitions than spatial encoding, and hence may be easier to incorporate into existing *n*D protocols and platforms. These advantages will be further explored within analytical chemical settings, in upcoming studies.

Acknowledgments

This research was supported by the Israel Science Foundation (ISF 447/09), the European Commission (EU-NMR contract No. 026145), by a Helen and Martin Kimmel Award for Innovative Investigation and by the generosity of the Perlman Family Foundation.

References

[1] D.M. Grant, R.K. Harris (Eds.), Encyclopedia of NMR, J. Wiley & Sons, Chichester, 1996.
[2] R.R. Ernst, G. Bodenhausen, A. Wokaun, Principles of Nuclear Magnetic Resonance in One and Two Dimensions, Clarendon, Oxford, 1987.
[3] J. Cavanagh, W.J. Fairbrother, A.G. Palmer, N.J. Skelton, Protein NMR Spectroscopy: Principles and Practice, Academic Press, Boston, 2007.
[4] J. Jeener, Lecture Presented at Ampere International Summer School II, Basko Polje, Yugoslavia, 1971.
[5] W.P. Aue, E. Bartholdi, R.R. Ernst, Two dimensional spectroscopy: application to nuclear magnetic resonance, J. Chem. Phys. 64 (1976) 2229–2246.
[6] S. Kim, T. Szyperski, GFT NMR, a new approach to rapidly obtain precise high-dimensional NMR spectral information, J. Am. Chem. Soc. 125 (2003) 1385–1393.
[7] D.P. Frueh, Z.-Y. Sun, D.A. Vosburg, C.T. Walsh, J.C. Hoch, G. Wagner, Non-uniformly sampled double-TROSY hNcaNH experiments for NMR sequential assignments of large proteins, J. Am. Chem. Soc. 128 (2006) 5757–5763.
[8] E. Kupce, R. Freeman, Hyperdimensional NMR spectroscopy, Prog. Nucl. Magn. Reson. Spectrosc. 52 (2008) 22–30.
[9] P. Schanda, Fast-pulsing longitudinal relaxation optimized techniques: Enriching the toolbox of fast biomolecular NMR spectroscopy, Prog. Nucl. Magn. Reson. Spectrosc. 55 (2009) 238–265.
[10] G. Liu et al., NMR data collection and analysis protocol for high-throughput protein structure determination, Proc. Natl. Acad. Sci. USA 102 (2005) 10487–10492.
[11] S.-T. Hsu, P. Fucini, L.D. Cabrita, H. Lannay, C.M. Dobson, J. Christodoulou, Structure and dynamics of a ribosome-bound nascent chain by NMR spectroscopy, Proc. Natl. Acad. Sci. USA 104 (2007) 16516–16521.
[12] D. Sakakibara et al., Protein structure determination in living cells by in-cell NMR spectroscopy, Nature 458 (2009) 102–105.
[13] L. Frydman, T. Scherf, A. Lupulescu, The acquisition of multidimensional NMR spectra within a single scan, Proc. Natl. Acad. Sci. USA 99 (2002) 15858–15862.
[14] L. Frydman, A. Lupulescu, T. Scherf, Principles and features of single-scan two-dimensional NMR spectroscopy, J. Am. Chem. Soc. 125 (2003) 9204–9217.
[15] M. Mishkovsky, L. Frydman, Principles and progress in ultrafast multidimensional NMR, Ann. Rev. Phys. Chem. 60 (2009) 429–448.
[16] P. Mansfield, Multi-Planar image formation using NMR spin echoes, J. Phys. C: Solid State Phys. 10 (1977) 55–58.
[17] P. Mansfield, Spatial mapping of the chemical shift in NMR, Magn. Reson. Med. 1 (1984) 370–386.
[18] D.B. Twieg, The k-trajectory formulation of the NMR imaging process with applications in analysis and synthesis of imaging methods, Med. Phys. 10 (1983) 610–621.
[19] A. Bax, A.F. Mehlkopf, J. Smidt, Fast method for obtaining 2D J-resolved absorption spectra, J. Magn. Reson. 40 (1980) 213–220.
[20] L. Frydman, J. Peng, Non-cartesian sampling schemes and the acquisition of 2D NMR correlation spectra from single-scan experiments, Chem. Phys. Lett. 220 (1994) 371–377.
[21] P. Blumler, J. Jansen, B. Blumich, Two-dimensional one-pulse rotational echo spectra, Solid State Nucl. Magn. Reson. 3 (1994) 237–240.
[22] D. Massiot, J. Hiet, N. Pellerin, F. Fayon, M. Deschamps, S. Steuernagel, P.J. Grandinetti, Two-dimensional one-pulse MAS of half-integer quadrupolar nuclei, J. Magn. Reson. 181 (2006) 310–315.
[23] G. Bodenhausen, D.J. Ruben, Natural abundance 15N NMR by enhanced heteronuclear spectroscopy, Chem. Phys. Lett. 69 (1980) 185–189.
[24] G.A. Morris, R. Freeman, Enhancement of nuclear magnetic resonance signals by polarization transfer, J. Am. Chem. Soc. 114 (1992) 10663–10665.
[25] L.E. Kay, P. Keifer, T. Saarinern, Pure absorption gradient enhanced heteronuclear single-quantum correlation spectroscopy with improved sensitivity, J. Am. Chem. Soc. 101 (1979) 760–762.
[26] M. Gal, M. Mishkovsky, L. Frydman, Real-time monitoring of chemical transformation by ultrafast 2D NMR spectroscopy, J. Am. Chem. Soc. 128 (2006) 951–956.
[27] L. Frydman, D. Blazina, Ultrafast two-dimensional nuclear magnetic resonance spectroscopy of hyperpolarized solutions, Nat. Phys. 3 (2007) 415–419.
[28] S. Bowen, C. Hilty, Time-resolved dynamic nuclear polarization enhanced NMR spectroscopy, Angew. Chem. Int. Ed. 120 (2008) 5313–5315.
[29] P. Pelupessy, Adiabatic single scan two-dimensional NMR spectroscopy, J. Am. Chem. Soc. 125 (2003) 12345–12350.